Inorganica Chimica Acta, 46 (1980) 139–146

The Kinetics of the Reaction of Aquo Fe(III) Myoglobin with Hydrogen Peroxide at pH 8

G. MARIUS CLORE, ANDREW N. LANE† and MICHAEL R. HOLLAWAY

Department of Biochemistry, University College London, Gower Street, London WC1E 6BT, U.K.

Received December 1, 1979

The kinetics of the reaction of aquo Fe(III) myoglobin (Mb(III)) with H_2O_2 at pH 8.0 and 20 °C have been investigated quantitatively under non-linear second order conditions. The data obtained at five concentrations of H_2O_2 (molar ratio $[H_2O_2]/[Mb]_{total}$ in the range 0.3 to 4) were analysed simultaneously by means of non-linear numerical integration and optimization techniques. The only mechanism that satisfied the triple requirement of a standard deviation within the standard error of the experimental data, good determination of the optimized parameters and a random distribution of residuals is as follows: Mb(III) reacts with H_2O_2 to form species X with a second order rate constant $k_{+1} = 3.53 \times 10^2$ M^{-1} s^{-1}; species X in turn reacts with H_2O_2 to form species R with a second order rate constant $k_{+2} = 3.40 \times 10^3$ M^{-1} s^{-1}; species R is then converted back into Mb(III) with a first order rate constant $k_{+3} = 9.60 \times 10^{-5}$ s^{-1}. At 408 nm $\Delta\epsilon_{Mb(III)-R} = 71.9$ mM^{-1} cm^{-1} and $\Delta\epsilon_{Mb(III)-X} = 104$ mM^{-1} cm^{-1}. Species R is spectrally identical to the Fe(IV) myoglobin species described by George and Irvine [Biochem. J., 52, *511–517 (1952)*]. *The chemical nature of species X and R is discussed on the basis of the data in the present paper and data in the literature from EPR, Mössbauer, resonance Raman and magnetic susceptibility studies.*

Introduction

As part of our continuing study on the reactivity of haem groups in simple redox reactions and the manner in which their reactivity may be modified by combination with different apoproteins [1–3], we have examined in detail the kinetics of the reaction of aquo Fe(III) myoglobin (Mb(III)) with H_2O_2.

The reactions of a number of haem proteins with H_2O_2 have been described and are well characterized in the case of horseradish peroxidase [4], cytochrome c peroxidase [5] and catalase [6], but only poorly so in the case of Mb(III). Spectroscopic [7, 8] and magnetic susceptibility [9] studies indicate that Fe(IV) species are formed, and kinetic investigations have shown that the apparent second order rate constants for the formation of these species differ by up to a factor of 10^5 within this series of haem proteins [10].

The reaction of Mb(III) with H_2O_2 in the pH range 8 to 9 results in the formation of a relatively stable red compound which we will call species R and which is characterized by an absorption maximum at 422 nm in the Soret region, together with a maximum at 547 nm, a weak band at 580–590 nm and a low shoulder at 510–520 nm in the α, β region [11–13]. At pH values below 8, a green compound is also formed and the products of the reaction are unstable; above pH 9, species R is converted to choleglobin in which the porphyrin ring has been oxidized [11, 12]. Redox titrations on species R demonstrated that the iron atom retained one oxidizing equivalent above the ferric state [11, 14]. Magnetic susceptibility [9], resonance Raman [8] and Mössbauer [7] studies on species R are consistent with the formulation of an Fe(IV) low spin, axially compressed t_{2g}^4 system in a $^3A_2$ ground state. The ligand in the sixth coordination position of the iron atom of species R is unknown.

The kinetics of the reaction of Mb(III) with H_2O_2 between pH 8 and 9 have been studied by a number of other workers, and although not fully characterized and understood, shown to be complex [11, 14–16]. However, a number of features of the reaction are known which put certain constraints on any proposed kinetic scheme. First, the complete conversion of Mb(III) to species R requires more than an equimolar amount of H_2O_2, and the relative amount of species R formed is dependent on the molar ratio of H_2O_2 to myoglobin and independent of the absolute concentrations of the reactants [11]. On the basis of these data George and Irvine [11] concluded that the formation of species R from Mb(III) and H_2O_2 proceeds by an irreversible process and does not occur by a single step mechanism. Second, under conditions of approximately stoichiometric concen-

†Present address: Biozentrum de Universität Basel, Abt. für Biophysikalische Chemie, Basle, Switzerland.

trations of reactants, the formation of a transient free radical species has been detected by EPR [14–16]. Third, O_2 is evolved and Mb(III) regenerated during the course of the reaction [15].

In the present paper we have analysed the kinetics of the reaction of Mb(III) with H_2O_2 at pH 8.0 under non-linear second order conditions (molar ratio $[H_2O_2]/[Mb]_{total}$ in the range 0.3 to 4) quantitatively by means of non-linear numerical integration and optimization techniques in order to obtain further insight into the mechanism of this reaction and the source of its complexity.

Experimental

Sperm whale myoglobin type III was purchased from Sigma. The solid myoglobin was dissolved in 0.05 *M* tris(hydroxymethyl)amino methane buffer pH 8.0, and, in order to ensure that all the myoglobin was in the ferric state, a five fold excess of $K_3Fe(CN)_6$ was added. The excess $Fe(CN)_6^{3-}$ and $Fe(CN)_6^{4-}$ was then removed by passage through a G-25 Sephadex column. The concentrations of myoglobin solutions were measured from the absorbance of the deoxy Fe(II) form at 556 nm which has a pH independent extinction coefficient of 11.8 mM^{-1} cm^{-1} [17] (the deoxy Fe(II) form is obtained by reduction of Mb(III) with trace amounts of sodium dithionite). Bovine liver catalase was purchased from Boehringer Mannheim and the concentration of catalase solutions calculated using $\epsilon_{405} = 340$ mM^{-1} cm^{-1} [18]. Hydrogen peroxide was purchased from BDH Chemicals Ltd.; before each experiment a stock solution of approx. 0.1 M was standardized against $KMnO_4$ using the method of Allen [19] and then diluted to the desired concentration. All reagents were of analytical grade.

Fast kinetics were observed used a single beam Durrum-Gibson stopped-flow spectrophotometer. Slow absorbance, charges and absorption spectra were recorded on a Cary Model 212 spectrophotometer.

The experimental data were digitized by the method of Clore and Chance [2]. The overall standard error of the data was 1.5 ± 0.2%. The kinetic data were analysed by means of non-linear stiff numerical integration and optimization techniques as described previously [2, 20, 21]. We minimize the normalized χ^2 given by

$$\chi^2 = \sum_{i=1}^{n} \sum_{j=1}^{m} R_{ij}^2 = \sum_{i=1}^{n} \sum_{j=1}^{m} \{(v_{ij} - u_{ij})/\sigma_i\}^2 \qquad (1)$$

where j identifies the time point and i the data curve, R_{ij} are the residuals, v_{ij} the observed values, u_{ij} the corresponding calculated value and σ_i the standard error of curve i. The overall standard deviation (S.D.) of the fit is then given by

$$\text{S.D.} = \Phi\{\chi^2/(d - p)\}^{1/2} \qquad (2)$$

where d is the total number of experimental points, p the number of optimized parameters and Φ the overall standard error of the data given by the weighted mean of the standard errors of the individual curves

$$\Phi = \Sigma\sigma_i r_i / \Sigma r_i \qquad (3)$$

where r_i is the range of curve i. A measure of the distribution of residuals for the overall fit is given by the mean absolute correlation index ($\bar{C}$):

$$\bar{C} = \frac{1}{n} \sum_{i=1}^{n} \left| \sum_{j=1}^{m} R_{ij} / \left(\sum_{j=1}^{m} R_{ij}^2 \right)^{1/2} \right| \qquad (4)$$

A value of $\bar{C}$ significantly greater than 1.0 (the expected root mean square value of $\bar{C}$ if the residuals for each curve were all independent random variables of zero mean and the same variance) indicates that the departures between calculated and observed values are systematic [2]. A quantitative measure of how accurately an optimized parameter has been determined is given by the standard deviation of its natural logarithm ($S.D._{ln}$). For values of $S.D._{ln} < 0.2$, $S.D._{ln} \approx \Delta x/x$, the relative error of the value of the parameter; for larger values of $S.D._{ln}$, up to 1 in magnitude, the parameter value is determined to within a factor $e \simeq 2.72$, and so its order of magnitude is known; significantly larger values of $S.D._{ln}$ show that the observations are inadequate to determine the parameter.

In order to analyse complex kinetic data, it is essential to have a set of strict quantitative criteria on which to base one's choice of model. Such criteria have been developed by Clore & Chance [2] and consist of the following triple requirement: an S.D. within the standard error of the data, good determination of the optimized parameters and a random distribution of residuals. Thus for a given set of data, although there may be many models with an S.D. within the standard error of the data, models with too many degrees of freedom will fail such an analysis because of under-determination, and models with too few degrees of freedom will fail such an analysis as a result of the introduction of systematic errors in the distribution of residuals.

Results

In Figs. 1 and 2 a series of progress curves for the reaction of Mb(III) with H_2O_2, monitored at 408 nm, are shown under conditions where the molar ratio $[H_2O_2]/[Mb]_{total}$ lies in the range 0.3 to 4. The conformity of the data to the kinetic schemes given in Table I was tested by fitting the numerical solution of the ordinary differential equations derived for each scheme to the six progress curves in Figs. 1 and

TABLE I. Schemes for the Reaction of Mb(III) with H_2O_2 together with their Overall Standard Deviations of the Fits and Mean Absolute Correlation Indices to the Data in Figs. 1 and 2.

Schemes B and C are analogous to the schemes for the reactions of horseradish peroxidase [4] and catalase [6] with hydrogen peroxide respectively. The mean absolute correlation index, $\bar{C}$, is a measure of the distribution of residuals and is defined by Eqn. (6). For $\bar{C} < 1.0$, the distribution of residuals is random; for $\bar{C} \gg 1.0$, the deviations between the computed and observed progress curves are systematic [2]. The overall standard error of the data in Figs. 1 and 2 is 1.5 ± 0.2% with a 99% confidence interval of 1.1–1.9%.

Scheme		S.D. (%)	$\bar{C}$
A.	$Mb(III) + H_2O_2 \xrightarrow{k_{+1}} X$ $X + H_2O_2 \xrightarrow{k_{+2}} R$ $R \xrightarrow{k_{+3}} Mb(III)$	1.2	0.98
B.[a,b]	$Mb(III) + H_2O_2 \underset{k_{-1}}{\overset{k_{+1}}{\rightleftharpoons}} R \xrightarrow{k_{+2}} Mb(III)$	4.8	3.2
C.[a]	$Mb(III) + H_2O_2 \underset{k_{-1}}{\overset{k_{+1}}{\rightleftharpoons}} R$ $R + H_2O_2 \xrightarrow{k_{+2}} Mb(III)$	5.4	3.3
D.[a]	$Mb(III) + H_2O_2 \underset{k_{-1}}{\overset{k_{+1}}{\rightleftharpoons}} R \begin{matrix} \xrightarrow{k_{+2}} Mb(III) \\ \xrightarrow{k_{+3}} Y \end{matrix}$	5.3	2.6

[a]The addition of an extra first order step such that [⇌ R →] is replaced by [⇌ X → R →] does not improve the S.D.'s of the fits of schemes B, C and D, and results in poor determination of some of the optimized parameters ($S.D._{ln} \gg 1$). [b]The addition of a minor species E* either independent of E or in equilibrium with E, and reacting with H_2O_2 by an identical mechanism to E but at a different rate, does not improve the S.D. of the fit of scheme B, and results in poor determination of some of the optimized parameters ($S.D._{ln} \gg 1$).

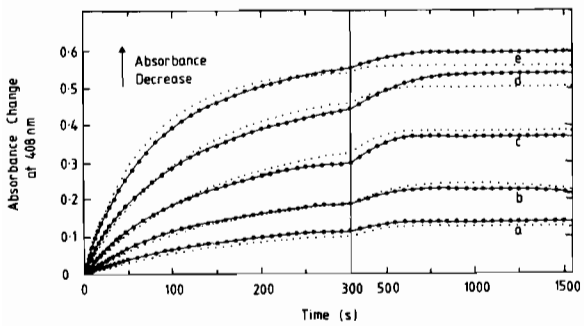

Fig. 1. Comparison of the observed (●) time courses at 408 nm for the reaction of Mb(III) with approximately stoichiometric concentrations of H_2O_2 with the best fit computed time courses for schemes A (——) and B (••••). 8.49 μM (final concentration) Mb(III) was dissolved in 0.05 M tris(hydroxymethyl)amino methane buffer pH 8.0 at 20 °C and reacted with (a) 2.78 μM, (b) 5.55 μM, (c) 11.1 μM, (d) 20.0 μM and (e) 35.1 μM (final concentrations) H_2O_2.

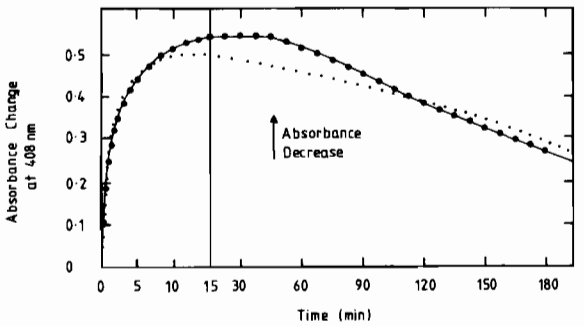

Fig. 2. Comparison of the observed (●) time course at 408 nm for the reaction of Mb(III) with an approximately stoichiometric concentration of H_2O_2 with the best fit time courses for schemes A (——) and B (••••) showing the decay phase of the reaction. 8.49 μM (final concentration) Mb(III) dissolved in 0.05 M tris(hydroxymethyl)amino methane buffer pH 8.0 at 20 °C, was reacted with 20.0 μM (final concentration) H_2O_2.

TABLE II. Optimized Values of the Parameters for Scheme A together with Their S.D.$_{ln}$ and 5–95% Confidence Limits.

Parameter	Dimensions	Value	S.D.$_{ln}$	Confidence limits	
				5%	95%
k_{+1}	M^{-1} s^{-1}	3.53×10^2	0.0163	3.43×10^2	3.62×10^2
k_{+2}	M^{-1} s^{-1}	3.40×10^3	0.0474	3.14×10^3	3.67×10^3
k_{+3}	s^{-1}	9.60×10^{-5}	0.0139	9.38×10^{-5}	9.82×10^{-5}
$\Delta\epsilon^{408}_{Mb(III)-X}$	M^{-1} cm^{-1}	1.04×10^5	0.0307	9.89×10^4	1.09×10^5
$\Delta\epsilon^{408}_{Mb(III)-R}$	M^{-1} cm^{-1}	7.19×10^4	0.0155	7.01×10^4	7.38×10^4

TABLE III. Optimized Values of the Parameters for Scheme B together with Their S.D.$_{ln}$ and 5–95% Confidence Limits.

Parameter	Dimensions	Value	S.D.$_{ln}$	Confidence limits	
				5%	95%
k_{+1}	M^{-1} s^{-1}	4.07×10^2	0.0159	3.96×10^2	4.18×10^2
k_{-1}	s^{-1}	8.08×10^{-4}	0.0595	7.32×10^{-4}	8.91×10^{-4}
k_{+2}	s^{-1}	2.26×10^{-4}	0.0394	2.12×10^{-4}	2.42×10^{-4}
$\Delta\epsilon^{408}_{Mb(III)-R}$	M^{-1} cm^{-1}	7.20×10^4	0.0160	7.01×10^4	7.39×10^4

2 simultaneously by means of non-linear optimization of the unknown parameters (*i.e.* rate constants and difference extinction coefficients). Only scheme A stated as

$$\begin{aligned} &Mb(III) + H_2O_2 \xrightarrow{k_{+1}} X \\ &X + H_2O_2 \xrightarrow{k_{+2}} R \\ &R \xrightarrow{k_{+3}} Mb(III) \end{aligned} \qquad (5)$$

satisfied the triple requirement ([2], see Experimental section) of a S.D. within the standard error of the data (*i.e.* $< 1.5\%$), good determination of the optimized parameters and a random distribution of residuals. The other kinetic schemes all failed on two counts: S.D. s greater than the standard error of the data and systematic errors in the distribution of residuals. The overall S.D. of the fit and the mean absolute correlation index (a measure of the nature of the distribution of residuals) for each scheme are given in Table I.

The optimized values of the rate constants and molar difference extinction coefficients at 408 nm of Mb(III) minus species X ($\Delta\epsilon^{408}_{Mb(III)-X}$) and Mb(III) minus species R ($\Delta\epsilon^{408}_{Mb(III)-R}$) for scheme A are given in Table II. The comparison of the experimental and computed progress curves for scheme A is shown in Figs. 1 and 2. The best fit curves for scheme B (which gave the second best fit after scheme A) are also shown in Figs. 1 and 2, and clearly demonstrate the presence of systematic errors between the observed and computed curves. The optimized values of the unknown parameters for scheme B are given in Table III.

The comparison of the experimental and computed dependence for schemes A and B of the normalized amplitude of the reaction (defined as the ratio of the maximum absorbance change produced in the reaction, ΔA^{408}_{max}, to the absorbance change produced by the complete conversion of Mb(III) to species R, $\Delta A^{408}_{Mb(III)-R}$) on the ratio $[H_2O_2]/[Mb]_{total}$ is shown in Fig. 3. As in the case of the progress curves in Figs. 1 and 2, systematic errors between the observed and computed curves for scheme B are seen. From Fig. 3 it can be seen that the dependence of the normalized amplitude of the reaction ($\Delta A^{408}_{max}/\Delta A^{408}_{Mb(III)-R}$) on the ratio $[H_2O_2]/[Mb]_{total}$ is non-linear and approaches a maximum of 1 when $[H_2O_2]/[Mb]_{total} \approx 4$. If the reaction proceeded by a single step irreversible second order mechanism (*i.e.* $Mb(III) + H_2O_2 \rightarrow R$) then the curve would be a straight line with a slope of 1 up to $[H_2O_2]/[Mb]_{total} = 1$, and thereafter a horizontal line.

The computed dependence for scheme A of $[R]_{max}/[Mb]_{total}$ and $[X]_{max}/[Mb]_{total}$ on the ratio $[H_2O_2]/[Mb]_{total}$ is also shown in Fig. 3. The curve for $[R]_{max}/[Mb]_{total}$ is sigmoid and reaches a maximum of 1 when $[H_2O_2]/[Mb]_{total} \approx 4$. The curve for $[X]_{max}/[Mb]_{total}$ reaches a maximum of 0.08 when $[H_2O_2]/[Mb]_{total} \approx 0.4$, and the value of $[X]_{max}/[Mb]_{total}$ remains unchanged for all higher values of $[H_2O_2]/[Mb]_{total}$.

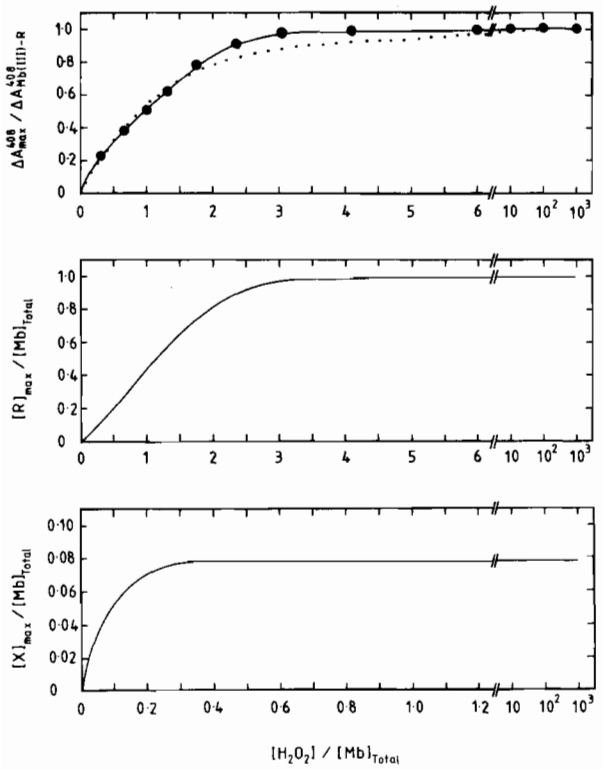

Fig. 3. Observed (●) and computed dependence for schemes A (——) and B (····) of the normalized amplitude of the reaction of Mb(III) with H_2O_2 at 408 nm ($\Delta A^{408}_{max}/\Delta A^{408}_{Mb(III)-R}$) on the molar ratio $[H_2O_2]/[Mb]_{total}$. The computed dependence for scheme A of $[R]_{max}/[Mb]_{total}$ and $[X]_{max}/[Mb]_{total}$ on the molar ratio $[H_2O_2]/[Mb]_{total}$ is also shown.

The computed time courses of Mb(III), species X, species R, H_2O_2 and C_{408} (the absorbance change at 408 nm in units of concentration) for scheme A are shown in Fig. 4 for $[H_2O_2]/[Mb]_{total} = 0.3, 1.0, 30$ and 100. A striking feature of this system which is seen throughout the H_2O_2 concentration range, is that only two species are present at the completion of the reaction: Mb(III) and species X, the latter only in small amounts. No species R, however, remains. This is not surprising as species R decays spontaneously to Mb(III) and requires the presence of H_2O_2 for its formation from species X.

The finding that the maximum concentration of species X reached during the reaction is small ($\leqslant 8\%$ of the total myoglobin concentration) due to the fact that $k_{+2} \gg k_{+1}$ has several consequences:

(1) The characterization of the optical spectrum of species X has not been possible.

(2) Providing species X is spectrally not too dissimilar from species R (*i.e.* $0.5 \leqslant \Delta\epsilon^{i}_{Mb(III)-X}/\Delta\epsilon^{i}_{Mb(III)-R} \leqslant 1.5$) repetitive wavelength scanning of the reaction at approximately stoichiometrically equal concentrations of H_2O_2 and myoglobin will yield a series of spectra with a single set of isosbestic points. This is confirmed in Fig. 5 where a single set of isosbestic points at 341 and 417 nm is observed in the Soret region.

(3) Under conditions of a large molar excess of H_2O_2 over myoglobin the progress curves of the reaction are monophasic and the kinetics are pseudo-first order up to high H_2O_2 concentrations (Fig. 6). The apparent second order rate constant corresponds to k_{+1} and from the data in Fig. 7 has a value of $3.5 \times 10^2\ M^{-1}\ s^{-1}$ which lies within the confidence limits of the value of k_{+1} found by non-linear optimization (Table II).

(4) The value of k_{+2} can only be found under conditions where the concentrations of H_2O_2 and myoglobin are approximately stoichiometric by non-linear optimization procedures.

As species R is immediately reformed from Mb(III) via species X in the presence of H_2O_2, the rate constant for the reaction

$$R \xrightarrow{k_{+3}} Mb(III) \qquad (6)$$

cannot be estimated from a semi-logarithmic plot of the decay phase of the reaction (see Fig. 2). Such a plot would yield a value of k_{+3} that was significantly underestimated. Thus, under these conditions the value of k_{+3} can only be determined by non-linear optimization. An accurate value of k_{+3}, however, may be obtained from a semi-logarithmic plot of the decay phase by removing all the remaining H_2O_2 by the addition of trace amounts of catalase ($[catalase]/[Mb]_{total} < 1/150$) after all the Mb(III) has been converted into species R. Catalase catalyses the overall reaction

$$2H_2O_2 \xrightarrow{k} 2H_2O + O_2 \qquad (7)$$

with an apparent second order rate constant $k \sim 4 \times 10^7\ M^{-1}\ s^{-1}$ [6] so that all the H_2O_2 present is removed rapidly (<5 min). Thus the only reaction observed approximately 5 min after the addition of catalase is the spontaneous reduction of species R to Mb(III) which proceeds by a first order process with a rate constant of $9.8 \times 10^{-5}\ s^{-1}$ determined from the semi-logarithmic plot in Fig. 7. This value of k_{+3} lies within the confidence limits of the value of k_{+3} obtained by non-linear optimization (Table II).

Discussion

The state of the iron atom in species R has been studied by Mössbauer [7], resonance Raman [8] and magnetic susceptibility [9] studies, all of which provide strong evidence for a low spin Fe(IV) state. Although the nature of the ligand in the sixth coordination position of the iron atom is unknown, several

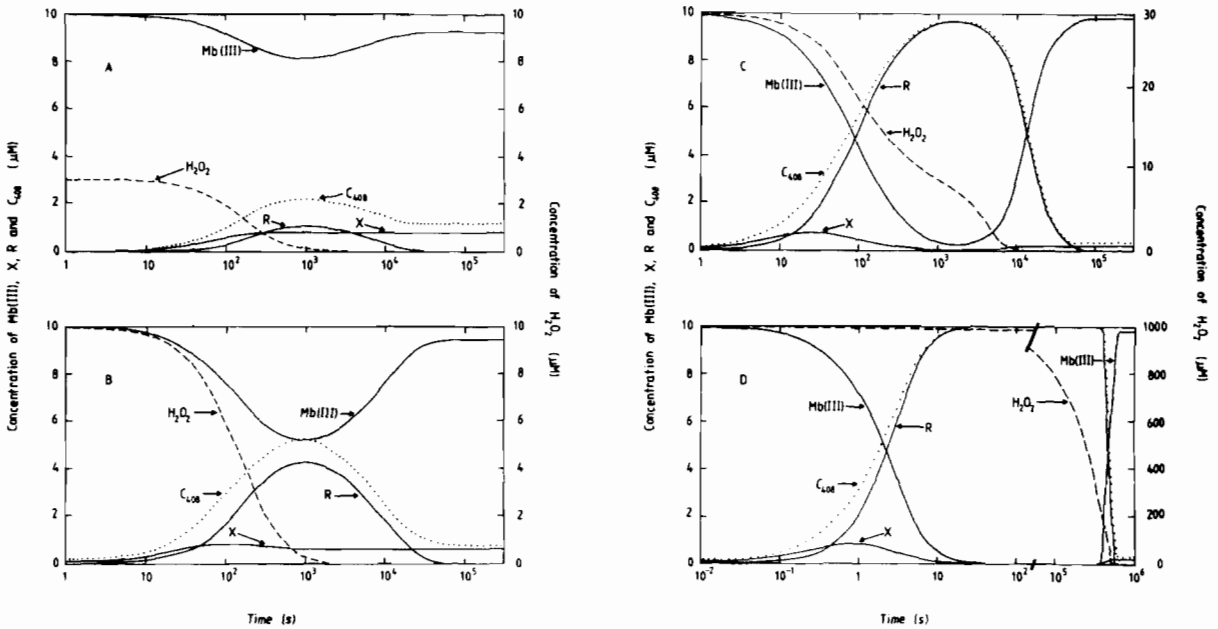

Fig. 4. Computed time courses of Mb(III), species X, species R, H_2O_2 and C_{408} (the absorbance change at 408 nm in units of concentration) for scheme A. The absorbance change in units of concentration, C_{408}, is given by $C_{408}(t) = [X(t)] \cdot \Delta\epsilon^{408}_{Mb(III)-X} / \Delta\epsilon^{408}_{Mb(III)-R} + [R(t)]$. The initial conditions are: [Mb(III)] = 10 μM; [H_2O_2] = 3 μM (A), 10 μM (B), 30 μM (C) and 1000 μM (D). The values of the rate constants, $\Delta\epsilon^{408}_{Mb(III)-X}$ and $\Delta\epsilon^{408}_{Mb(III)-R}$ are given in Table II.

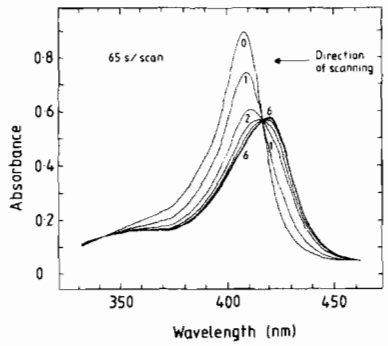

Fig. 5. Successive spectra in the Soret region illustrating the reaction of Mb(III) with H_2O_2. 5.84 μM (final concentration) Mb(III) dissolved in 0.05 M tris(hydroxymethyl)amino methane buffer pH 8.0 at 20 °C was mixed with 56.8 μM (final concentration) H_2O_2 (the total reaction volume was 3 ml, and the volume and concentration of the added H_2O_2 were 25 μl and 6.87 mM respectively). Spectra were recorded in a continuous repetitive scanning mode from right to left at a rate of 65 s per scan (*i.e.* 2 nm s^{-1}). Spectrum 0 is Mb(III) before the addition of H_2O_2.

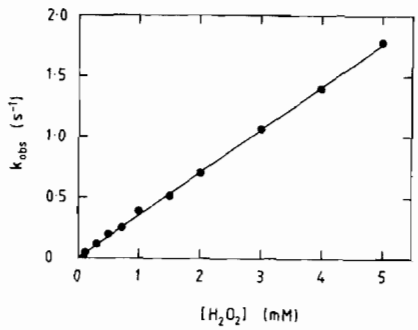

Fig. 6. Dependence of the pseudo-first order rate constant, k_{obs}, on the concentration of H_2O_2 for the reaction of Mb(III) with a large excess of H_2O_2. 10 μM Mb(III) in 0.05 M tris(hydroxymethyl)amino methane buffer pH 8.0 at 20 °C (syringe 1) was reacted with H_2O_2 dissolved in the same buffer (syringe 2) in the stopped flow apparatus. Semi-logarithmic plots of the progress curves were linear for more than 95% of the reaction. The wavelength monitored was 408 nm.

of its features may be deduced. O_2 is evolved during the reaction of Mb(III) with H_2O_2 and its evolution exhibits an appreciable lag phase in relation to the formation of species R [15] which indicates that O_2 is evolved during the spontaneous first order reduction of species R to Mb(III). This suggests that the ligand in the sixth coordination position contains two atoms of oxygen.

The observation of an EPR detectable transient free radical species at g ~ during the reaction of Mb(III) with H_2O_2 reaching a maximum spin concentration of approximately 10% of the total myoglobin concentration [14] may be correlated to species X. Given that the OH radical would be

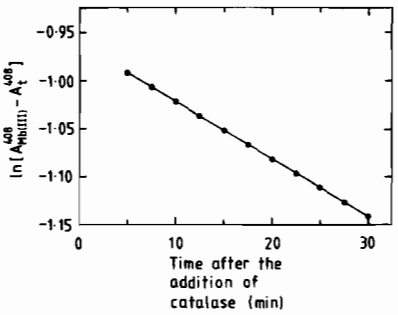

Fig. 7. Semi-logarithmic plot of the spontaneous reduction of species R to Mb(III) following the addition of trace amounts of catalase to remove all remaining H_2O_2. 5.8 μM (final concentration) Mb(III) dissolved in 0.05 M tris(hydroxymethyl) amino methane buffer pH 8.0 at 20 °C was allowed to react with 92 μM (final concentration) H_2O_2 until the absorbance change at 408 nm reached a maximum and all the myoglobin was in the form of species R (~10 min). 0.036 μM (final concentration) catalase was then added and the subsequent reduction of species R to Mb(III) monitored at 408 nm.

expected to be undectable owing to its very short lifetime at room temperature (the reaction $OH^{\bullet} + OH^{\bullet} \rightarrow H_2O_2$ proceeding with a second order rate constant of $5.5 \times 10^9\ M^{-1}\ s^{-1}$ [22]), it seems likely that the free radical is either a protein cation radical as in cytochrome c peroxidase [5] or a porphyrin π-cation radical. In the latter case, unlike in compound I of horseradish peroxidase [4], the electron localized on the porphyrin would not be coupled through exchange interactions with spin localized on the haem iron, thereby accounting for the presence of a $g \sim 2$ EPR signal. The spectral similarity in the Soret region of species X and R deduced from Fig. 5 (see Results section) suggests that the iron atom in both species is in the same formal valence state, namely Fe(IV).

The observation in unbuffered solutions that the formation of species R is accompanied by the release of one proton [23] indicates that ionizing groups in the active site are involved in the reaction of Mb(III) with H_2O_2.

On the basis of our kinetic analysis and the above evidence, we suggest the following mechanism for the reaction of Mb(III) with H_2O_2 at pH 8.0. The first step is a two electron transfer reaction resulting in the oxidation of Mb(III) to species X:

$$\begin{matrix}\left[\begin{matrix}B_1H\\ Fe^{3+}\\ Z\\ B_2H\end{matrix}\right.\end{matrix} + H_2O_2 \xrightarrow[3.53 \times 10^2\ M^{-1}\ s^{-1}]{k_{+1}} \left[\begin{matrix}B_1^-\\ Fe^{4+}\cdot OH^-\\ Z^{+\bullet}\\ B_2H\end{matrix}\right. + H_2O \qquad (8)$$

Mb(III) species X

where Z represents either an amino acid in the active site or the porphyrin, $Z^{+\bullet}$ is the cation free radical produced by the oxidation of Z, and B_1H and B_2H are ionizing groups in the active site. The second step is a one electron reduction of species X by H_2O_2 resulting in the formation of species R:

$$\begin{matrix}\left[\begin{matrix}B_1^-\\ Fe^{4+}\cdot OH^-\\ Z^{+\bullet}\\ B_2H\end{matrix}\right.\end{matrix} + H_2O_2 \xrightarrow[3.40 \times 10^3\ M^{-1}\ s^{-1}]{k_{+2}} \left[\begin{matrix}B_1^-\\ Fe^{4+}\cdot OOH\\ Z\\ B_2^-\end{matrix}\right. + H_2O + H^+ \qquad (9)$$

species X species R

As $Fe^{4+}\cdot OOH$ is of integral spin, no EPR signals are seen in species R [24]. It should be noted that the configuration $Fe^{4+}O_2^-$ for species R can be excluded as it would be expected to exhibit an EPR signal. In the third step, species R undergoes an internal oxidation-reduction reaction resulting in the reduction of Fe^{4+} to Fe^{3+} and the oxidation of the liganded $\cdot OOH$ to O_2:

$$\begin{matrix}\left[\begin{matrix}B_1^-\\ Fe^{4+}\cdot OOH\\ Z\\ B_2^-\end{matrix}\right.\end{matrix} \xrightarrow[+H^+]{k_{+3},\ 9.60 \times 10^{-5}\ s^{-1}} \left[\begin{matrix}B_1H\\ Fe^{3+}\\ Z\\ B_2H\end{matrix}\right. + O_2 \qquad (10)$$

species R Mb(III)

The overall stoichiometry of the reaction of Mb(III) with H_2O_2 corresponds to that of the classical scheme for the reaction of ferric catalase with H_2O_2 given by [25]:

$$Cat(Fe^{3+}) + H_2O_2 \underset{k_{-1}}{\overset{k_{+1}}{\rightleftharpoons}} \text{compound I } (Z^{+\bullet}Fe^{4+})$$

$$\text{compound I} + H_2O_2 \xrightarrow{k_{+2}} Cat + 2H_2O + O_2 \qquad (11)$$

Thus, it is useful to compare and contrast the two systems.

The first step in the reactions of both Mb(III) and ferric catalase with H_2O_2 appears to involve a direct two electron transfer resulting in the formation of an intermediate two oxidizing equivalents above Mb(III) and ferric catalase: species X in the case of the Mb(III) reaction and compound I [6] in the catalase reaction. The second order rate constant for the formation of species X is smaller than that for the formation of compound I by a factor of about 10^5 (*cf.*

Table II and ref. 25). This difference may be due to steric factors imposed by the apoprotein limiting access of H_2O_2 to the iron atom. This view is supported by the observation that the rate constants for the formation of complexes between Mb(III) and small ligands are in general much smaller than those for the corresponding reactions with ferric catalase [26].

In the second stage of the catalase reaction O_2 is evolved and ferric catalase regenerated in a process that appears to involve only a single step (*i.e.* an apparent direct two electron reduction of compound I) as far as can be determined from kinetic measurements [6, 10, 25]. If a species corresponding to species R (*i.e.* a compound II-like species) is an intermediate in the catalase reaction, then, given that the overall reaction is second order up to a concentration of 1 *M* H_2O_2 and $k_{+2}^{app} \sim 2 \times 10^7 M^{-1} s^{-1}$ [25], the rate constant (k_{+3}) for its breakdown must be greater than 10^8 s^{-1}. Thus, if the reactions of ferric catalase and Mb(III) with H_2O_2 proceed by similar mechanisms, this would give a 10^{12} fold difference in the stability of the respective R species (as $k_{+3} \sim 10^{-4}$ s^{-1} in the Mb(III) system). On the other hand if the catalase reaction does indeed proceed by a mechanism involving a direct two electron reduction of compound I by H_2O_2, then the importance of the apoprotein in transforming the reactivity of the haem group in catalase away from that in the 'model' Mb(III) system is even further emphasized.

Acknowledgements

We wish to thank the Science Research Council for financial support. A.N.L. acknowledges the receipt of an S.R.C. studentship.

References

1 R. P. Cox and M. R. Hollaway, *Eur. J. Biochem.*, *74*, 575 (1977).
2 G. M. Clore and E. M. Chance, *Biochem. J.*, *173*, 799 (1978).
3 G. M. Clore, L. E. Andreasson, B. Karlsson, R. Aasa and B. G. Malmström, *Biochem. J.*, *185*, 1 (1980).
4 H. B. Dunford and J. S. Stillman, *Coord. Chem., Rev.*, *19*, 187 (1976).
5 T. Yonetani, in 'The Enzymes', 3rd edn. (P. D. Boyer, ed.), vol. 13, pp. 345–361, Academic Press, New York (1976).
6 G. R. Schonbaum and B. Chance, in 'The Enzymes', 3rd ed. (P. D. Boyer, ed.), vol. 13, pp. 362–408, Academic Press, New York (1976).
7 T. Harami, Y. Maeda, Y. Morita, A. Trautwein and U. Gonser, *J. Chem. Phys.*, *67*, 1164 (1977).
8 J. R. Campbell, R. J. H. Clark, G. M. Clore and A. N. Lane, *Inorg. Chim. Acta*, in the press.
9 A. Ehrenberg, in 'Hemes and Hemoproteins' (B. Chance, R. W. Estabrook and T. Yonetani, eds.) pp. 331–337, Academic Press, New York (1966).
10 J. M. Pratt, in 'Techniques and Topics in Bio-inorganic Chemistry' (C. A. McAuliffe, ed.) pp. 107–206, MacMillan Press, London (1975).
11 P. George and D. H. Irvine, *Biochem. J.*, *52*, 511 (1952).
12 J. B. Fox, R. A. Nicholas, S. A. Ackerman and C. E. Swift, *Biochemistry*, *13*, 5178 (1974).
13 J. B. Wittenberg, *J. Biol. Chem.*, *253*, 5694 (1978).
14 T. Yonetani and H. Schleyer, *J. Biol. Chem.*, *242*, 1974 (1967).
15 N. K. King and M. E. Windfield, *J. Biol. Chem.*, *238*, 1520 (1963).
16 N. K. King, F. D. Looney and M. E. Windfield, *Biochim. Biophys. Acta*, *133*, 65 (1967).
17 E. Antonini and M. Brunori, 'Hemoglobin and Myoglobin and Their Reactions with Ligands', Elsevier–North Holland, Amsterdam (1971).
18 B. Chance, *J. Biol. Chem.*, *179*, 1299 (1949).
19 N. Allen, *Ind. Eng. Chem., Anal. Ed.*, *2*, 55 (1930).
20 E. M. Chance, A. R. Curtis, I. P. Jones and C. R. Kirby, *A.E.R.E. Report No.* R. 8775, A.E.R.E., Harwell (1977).
21 A. R. Curtis, *A.E.R.E. Report No.* R. 9352, A.E.R.E., Harwell (1979).
22 J. Robaini and M. S. Matheson, *J. Chem. Phys.*, *70*, 761 (1966).
23 J. Peisach, W. E. Blumberg, R. A. Wittenberg and J. B. Wittenberg, *J. Biol. Chem.*, *243*, 1871 (1968).
24 P. George and D.H. Irvine, *Biochem. J.*, *60*, 596 (1955).
25 B. Chance, D. S. Greenstein and F. J. W. Roughton, *Arch. Biochem. Biophys.*, *37*, 301 (1952).
26 A. N. Lane, *Ph. D. Thesis*, University of London (1979).